DETECTION OF ALONG-TRACK GROUND MOVING TARGETS IN HIGH RESOLUTION SPACEBORNE SAR IMAGES

D. Weihing [a], S. Hinz [a], F. Meyer [b], A. Laika [a], R. Bamler [a,b]

[a]Technical University of München, Remote Sensing Technology,
Arcisstr. 21, 80333 München,
(Diana.Weihing, Stefan.Hinz, Andreas.Laika)@bv.tum.de

[b]German Aerospace Center (DLR), Remote Sensing Technology
Oberpfaffenhofen, 82234 Wessling, Germany
(franz.meyer, richard.bamler)@dlr.de

Commission VII, Working Group VII/2

KEY WORDS: Radar, SAR, Detection, Estimation, Monitoring, Processing

ABSTRACT:

Future high resolution multi-aperture SAR satellites entail high potential for large-area traffic monitoring from space. While many approaches for detecting across-track moving vehicles in SAR images have already been published within the recent years, the detection of objects moving in along-track is still an issue to be solved. This paper deals with the detection of vehicles, mainly moving in along-track, in high resolution SAR images. The blurring effect caused by the along-track motion component is exploited for this detection scheme. The presented approach is based on a matched filter bank where the SAR image is processed with different matched filters. To extract a particular moving object from the filter bank, a specialized peak detector is employed. The proposed technique is demonstrated using data of an airborne SAR system (E-SAR from the DLR) and its potential is analyzed.

KURZFASSUNG:

Für grossflächige Verkehrsüberwachung bieten sich zukünftige hochaufgelöste SAR-Aufnahmen an. Während in den letzten Jahren verschiedene Ansätze zur Detektion von Fahrzeugen, die sich in across-track bewegen, veröffentlicht wurden, ist die Detektion von Fahrzeugen in along-track ein noch zu lösendes Problem. In diesem Artikel wird ein Ansatz zur Detektion von Fahrzeugen, hauptsächlich in along-track fahrend, in SAR Bildern präsentiert. Der sogenannte Verschmierungseffekt eines Objektes, verursacht von dessen Bewegung in along-track, wird hierfür herangezogen. Der Ansatz basiert auf der Verwendung von unterschiedlichen Filtern zur Fokussierung des SAR Bildes. Um ein Bewegtobjekt aus dem Stapel der unterschiedlich fokussierten Bilder zu extrahieren, wird ein spezialisierter Peak-Detektor verwendet. Anhand von flugzeuggetragenen SAR Daten (E-SAR von DLR) wird diese Methode veranschaulicht und das Potential dieses Ansatzes analysiert.

1. INTRODUCTION

1.1 Motivation

Since the amount of traffic is rapidly increasing, traffic monitoring and traffic control has become an important task over the past years. In order to get information about the situation on the whole road network and using them for prediction, a simultaneous observation of a large area is necessary. Therefore, images of spaceborne high-resolution SAR sensors can be a solution for nationwide traffic monitoring. With the launch of the German SAR satellite TerraSAR-X in 2006 a step forward towards spaceborne traffic monitoring will be possible. Satellite SAR images up to 1 m resolution will be available. In addition to high resolution, it is planned to provide also a Dual Receive Antenna mode, which enables interferometric measurements for detection of moving targets.

1.2 Related work

Detection of vehicles and estimation of their velocities are a challenging task. Moving targets suffer from special effects in the SAR processing algorithm and are not imaged like stationary scatterers. Hence, specific methods for detecting vehicles and estimating their location and motion parameters are required. The task of detecting cars and estimating the velocity with SAR has been treated in several publications, whereas the main emphasis was put on detection. Depending on the number of apertures, these methods can be grouped into several classes. If more than two channels are available for Ground Moving Target Indication (GMTI), as in most military systems, the use of Space Time Adaptive Processing (STAP) is the optimal method for distinguishing clutter from moving objects (Ender, 1999). In the case of two-channel systems, like TerraSAR-X or the Canadian Radarsat-2, some interferometric approaches can be used for detecting vehicles. Along-Track Interferometry (ATI) (Sikaneta and Gierull, 2005) and the so-called Displaced Phase Center Array (DPCA) method are the most prominent among them. For the ATI technique an interferogram has to be formed from the two SAR images by complex conjugate multiplication, in which the interferometric phase is related to the object motion. The detection is done based on a constant false alarm rate scheme, where probability density functions depending on the interferometric phase and the amplitude are used (Gierull, 2002). In DPCA processing the two SAR images are subtracted from each other and the magnitude of the result is evaluated for detection. Hence, the pdfs simplify to a one-dimensional case. These approaches have been extended by integrating a priori information, such as GIS data of road networks, in (Meyer *et al.*, 2005). In this concept some premises are exploited such as that vehicles are bound

to streets, which might not be true in military GMTI.

However, these interferometric detection algorithms can only be applied if the motion of the vehicle affects the interferometric phase, which is not the case if vehicles are moving in along-track. Gierull and Sikaneta (2004) applied filterbanks with matched filters to estimate ground moving parameters also for vehicles driving in along-track.

The presented approach in this paper is also based on a filterbank. However, in contrast to the above approaches a specialized peak detector is put on top of the filterbank for detection of vehicles.

In the next section an overview of the different effects moving vehicles cause in SAR images is given. The technique of using filterbanks, which is the basis of the presented approach, is described and afterwards the new detector is explained in Sect. 3. The performance of this FM rate detector is analysed using experimental airborne SAR data (E-SAR from the DLR).

2. THEORY OF MOVING OBJECTS IN SAR IMAGES

In an air- or spaceborne SAR imaging process a radar scans the earth in a side-looking fashion during its flight over the scene. While the sensor is moving it transmits microwave pulses at constant intervals given by the Pulse Repetition Frequency (PRF) and receives the echoes. In Fig. 1 the geometry of an image acquisition is shown. The radar is flying in a certain altitude h along the x-axis, also referred to azimuth direction or along-track. The y-axis, which is oriented perpendicular to the flight path, is usually refered to as Range or across-track direction. The position of the sensor at a certain point of time is given by $P_{sat}(t) = [x_{sat}(t), y_{sat}(t), z_{sat}(t)]$ and the location of the moving target by $P_{target} = [x_{mover}(t), y_{mover}(t), z_{mover}(t)]$. The distance between sensor and target corresponds to:

$$R(t) = P_{sat}(t) - P_{target}(t) \tag{1}$$

Herewith, $R_0 = \sqrt{y_0^2 + H^2}$ is the distance at $t = 0$ (the shortest range between SAR and target).

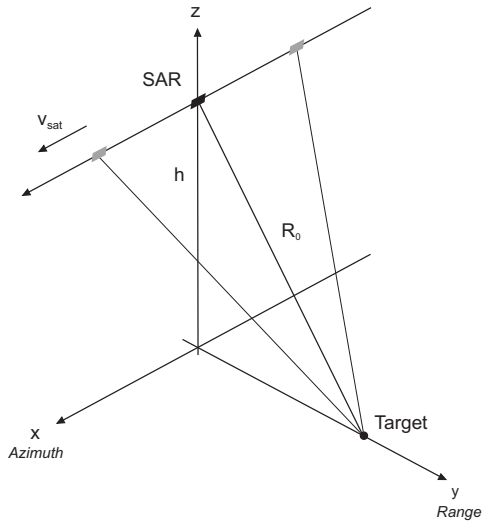

Figure 1. Imaging geometry of a spaceborne SAR

The received echo is a replica of the transmitted signal backscattered from the ground. For a detailed representation of the echo signal see (Bamler and Schättler, 1993). Here the received echo signal is simplified without loss of generality and can be written as:

$$h(t) = exp(-j\frac{4\pi}{\lambda}R(t)) = exp(j\pi FMt^2) \tag{2}$$

where $FM = -\frac{2}{\lambda}\frac{v_{sat}v_b}{R_0}$ is the frequency modulation rate of the azimuth chirp.

To form a SAR image out of the received echoes a matched filter algorithm is applied. The filter for azimuth focusing is defined by:

$$s(t) = exp(-j\pi FMt^2) \tag{3}$$

To circumvent an extensive convolution in time-domain, the operation is done in the frequency-domain by multiplicating the spectra of echos signal and filter.

$$U(f) = H(f) \cdot S(f) \tag{4}$$

However, for this process a stationary-world matched filter is assumed. Significantly moving and even accelerating objects violate this assumption and therefore the target will not be imaged "correctly". The dependencies on object velocity and acceleration components can be seen when expanding the range equation $R(t)$ into a third order Taylor series:

$$\begin{aligned} R(t) = R_0 + \frac{y_0 v_{y_0}}{R_0}t + \\ \frac{1}{2R_0}\left[(v_{x_0} - v_{sat})^2 + v_{y_0}^2\left(1 - \frac{y_0^2}{R_0^2}\right) + y_0 a_{y_0}\right]t^2 + \\ \frac{1}{2R_0}\left[v_{y_0}a_{y_0}\left(1 - \frac{y_0^2}{R_0^2}\right) + (v_{x_0} - v_{sat})a_{x_0}\right]t^3 - \\ \frac{1}{2R_0}\left[\frac{y_0 v_{y_0}(v_{x_0} - v_{sat})^2 + y_0 v_{y_0}^3}{R_0^2}\right]t^3 \end{aligned} \tag{5}$$

where v_{x_0} and v_{y_0} are the components of target's velocity in along- or across-track, respectively, and a_{x_0} and a_{y_0} the accelerations in these directions, each at the time $t = 0$. The imaging effects caused by the uncompensated motion parameters are explained in the following Sections.

2.1 Motion in across-track

The object is assumed to move in across-track with a constant velocity. This results in a linear change of the range history, so that the shortest distance is not at time $t = 0$ anymore, is shifted depending on the velocity in line-of-sight $v_{los} = v_{y_0} \cdot sin(\theta)$, with θ being the local elevation angle. Therefore, the echo signal of the moving target can be written as:

$$h_{mt_{across}}(t) = exp(j\pi FMt^2) \cdot exp(-j\frac{4\pi}{\lambda}v_{los}t) \tag{6}$$

The spectrum of the moving target after focusing with a stationary-world matched filter looks like:

$$U_{mt_{across}}(f) = \exp(-j2\pi \frac{2}{\lambda FM} f v_{los}) \exp(-j2\pi \frac{2}{\lambda^2 FM} v_{los}^2) \quad (7)$$

According to the correspondencies of the Fourier Transform the linear phase causes a shift in time domain. The shift in time-domain is $t_{shift} = \frac{2v_{los}}{\lambda FM}$ and can also be expressed in meters: $\Delta_{azimuth} = -R\frac{v_{los}}{v_{sat}}$. This means the vehicle gets displaced in the image in azimuth direction depending on its line-of-sight velocity.

2.2 Motion in along-track

Now the target should move in azimuth with constant velocity. Along-track motion changes the relative velocity between sensor and scatterer $(v_{x_0} - v_{sat})$ (cf. Equ. (5)) leading to a change of the quadratic part of the range history. A change of the quadratic component corresponds to a change of the FM rate according to:

$$\begin{aligned} FM_{mt} &= -\frac{2}{\lambda R}\left(\sqrt{v_{sat}v_B} - \sqrt{\frac{v_{sat}}{v_B}}v_{x0}\right)^2 \\ &= FM\left(1 - \frac{v_{x0}}{v_B}\right)^2 \end{aligned} \quad (8)$$

With the new FM rate FM_{mt} the echo signal results in:

$$h_{mt_{along}}(t) = exp(j\pi FM_{mt} t^2) \quad (9)$$

Focusing $h_{mt_{along}}(t)$ with a stationary world matched filter (SWMF) does not fully compensate for the quadratic phase term leading to a spread of the received signal corresponding to:

$$U_{mt_{along}}(f) = \exp(-j\pi \frac{f^2}{\delta FM}) \quad (10)$$

where $\frac{1}{\delta FM} \approx -\lambda\sqrt{\frac{v_{sat}}{v_B}}\frac{v_{x0}}{(v_{sat}v_B)^{\frac{3}{2}}}R$. Considering the stationary phase approximation the width of the focused peak can be approximated by:

$$\Delta t \approx \frac{PRF}{\delta FM} = 2T_A\frac{v_{x0}}{v_B} \quad (11)$$

Interpretating this equation shows that a target gets smeared twice the way it moved during the time of illumination T_A.

2.3 Acceleration in across-track

Like the component of along-track motion, acceleration in across-track mainly affects the quadratic part of Equ. (5). Hence, the acceleration in range also causes a spreading of the energy and the target will be smeared in azimuth. The crosstalk of along-track motion and across-track acceleration hampers the interpretability of along-track smearing without having additional information available.

2.4 Acceleration in along-track

Acceleration in along-track appears in the cubic term of the range history (cf. Equ. (5)), which causes an assimetry of the focused point spread function. However, for TerrSAR-X these effects are neglible (Hinz *et al.*, 2005).

The effects caused by across-track and along-track motion as well as across-track accelaration reach significant values when plugging the TerraSAR-X instrument parameters into the above formulae. We refer the reader to (Hinz *et al.* 2005, Meyer *et al.* 2005) for a detailed analysis of these effects regarding TerraSAR-X.

3. FM RATE DETECTOR

The "conventional" interferometric detection algorithms described in Sect. 1.2 can only be applied if significant displacement or interferometric phase values occur. For vehicles moving almost in along-track this is usually not the case. Hence, another technique must be utilized to detect moving objects under those circumstances.

As shown in Sect. 2.2 targets moving in along-track get blurred in the SAR image. However, it is possible to focus the moving object by choosing the correct FM rate for image processing, i.e. a FM rate is choosen, which corresponds to the realtive velocity between sensor and vehicle. To find the correct FM rate not only one but a stack of images is processed with varying FM rates. Figure 2 illustrates a stack of SAR images processed in such a way. The corresponding FM rate is found by searching for a focussed peak in the FM-azimuth plane of Fig. 2. Every FM-azimuth slice picks out a certain azimuth line (e.g. red line) from every image. A slice consisting of these azimuth lines arranged in order of the FM rates may look like Fig. 3.

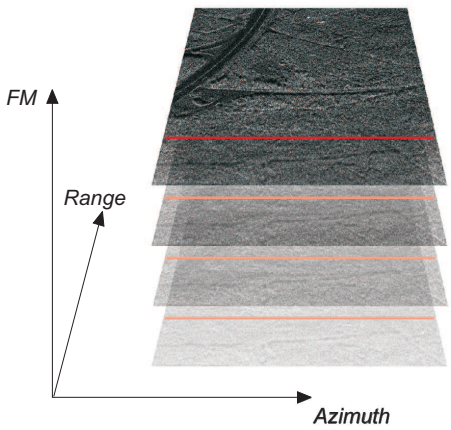

Figure 2. Stack of SAR images focused with different FM rates. For one azimuth line (red) a slice is built out of this line in every image

Restricting the search to one FM-azimuth slide is valid, as the blurring of moving objects only occurs in azimuth direction. However, a vehicle could still be distributed over more than one range cells. Therefore, the search domain has to be extended to a third dimension. If in slices of adjacent azimuth lines peaks are found at corresponding positions, an extended search in azimuth and

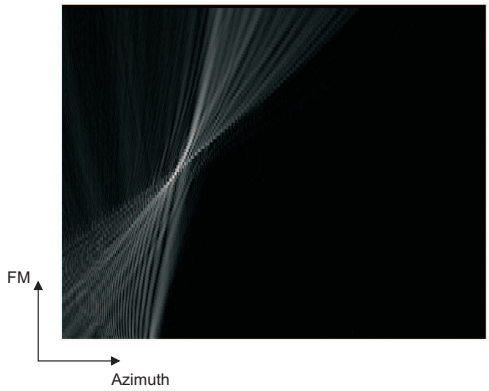

Figure 3. FM-azimuth slice for a moving target

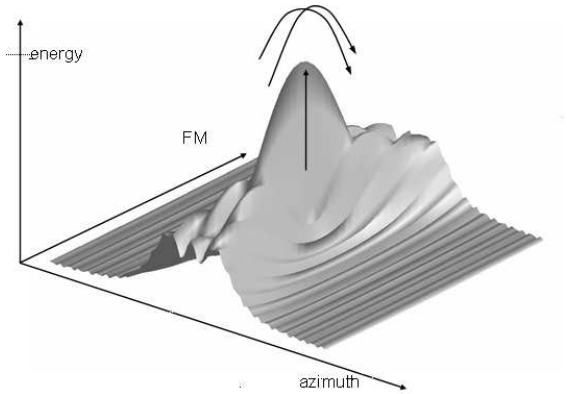

Figure 4. Analytical FM-azimuth sharpness function

range is done in the corresponding SAR image to estimate the final Range position. However, so far the search for the peak is still separated in two 2D-searches. The implementation of a real 3D search is in progress.

For stationary points, the energy peak of this "sharpness function" in the FM-azimuth slice (e.g. Fig. 3) is located at this FM rate where the reference along-track velocity was assumed to be 0 km/h (here the central row of the slice). The faster an object moves, the more the energy peak deviates from this row.

For extracting the energy peak, an algorithm must be applied to find the peak of the sharpness function even in the presence of disturbances like speckle or bright background clutter. Therefore, a blob detection scheme is implemented that analyzes the local curvatures in azimuth- and FM-direction (Hinz, 2005). This scheme is illustrated in Fig. 4 by an analytical and noise-free simulation of the sharpness function. The features used in this blob detection scheme are signed curvatures in azimuth and in FM direction and the mean energy in FM direction. The curvatures, which are restricted to a negative value, correspond to the directional second derivatives and must be estimated from the discrete data. Therefore, smoothing is advisable. The smoothing and the calculation of the second derivative are integrated into a Gaussian kernel:

$$gauss''_{\sigma}(x) = \frac{x^2 - \sigma^2}{\sigma^5 \cdot \sqrt{2\pi}} \cdot exp(-\frac{x^2}{2\sigma^2}) \tag{12}$$

The value for σ is not identical for the FM and azimuth direction, as they are differently sampled. A peak is defined by three conditions. It must hold a high absolute curvature value in azimuth direction I_{azaz}, a high absolute curvature value in FM direction I_{FMFM}, and a strong brightness in FM direction $I_{energy}(FM, azimuth = constant) = I_{energy}(FM)$. Combining local curvature maxima and energy amplitude by the geometric mean yields the final decision function, from which the maximum is selected:

$$pos(FM, azimuth) = \sqrt[3]{\frac{I_{azaz}}{c_{az}} \cdot \frac{I_{FMFM}}{c_{FM}} \cdot \frac{I_{energy}(FM)}{c_{energy}}} \tag{13}$$

with c being normalized constants. Before starting the peak search, a region of interest is specified. This region of interest is defined by selecting a certain percentage of the brightest pixels. Within this region $pos(FM, azimuth)$ is calculated and the maximum selected.

If a peak has been found, the velocity may be derived since the FM rate depends on the relative along-track velocity. However, acceleration in across-track has to be taken into account since it has the same blurring effect on the imaged vehicle. The crosstalk of the two effects affects the velocity estimation even for small heading angles with a small across-track component. The influence of accelerations on velocity estimation is discussed in detail in (Sharma *et al.*, 2006).

4. RESULTS

The proposed approach is tested on real SAR data. Therefor a scene at Gilching (A96) imaged by DLR's E-SAR system is used. The data of this flight campaign has been analyzed with the FM rate detector and some examples of the results are shown in the following. In Fig. 5 one can see a SAR image including the motorway A96 heading in along-track. The airplane was flying from bottom to the top of the image and recorded the data in a right-looking geometry. The red rectangle marks the azimuth line (or rather the part of it) which was extracted of every image of the FM stack to create the FM-azimuth slice. This slice is shown in Fig. 6. The left axis shows the corresponding FM rate in $[\frac{1}{s^2}]$ and the right axis represents the corresponding target azimuth velocity if acceleration effects can be ignored. The position of the detected peak is marked with a red circle. Around the peak the matched filter responses shift away from the peak position in azimuth, which may be caused by an across-track motion component or a squint during the data acquisition. The sharpness function is tilted and fans out caused by a mismatch of the linear component of matched filter and echo signal.

The corresponding FM-azimuth slice for the azimuth line framed with the cyan rectangle is shown in Fig. 7. Three peaks were detected, whereas only two apparently seem to be correct. The peak FM rate corresponds to target velocities of -51 km/h twice and -35 km/h if acceleration effects can be ignored.

Figure 8 shows a fragment of another SAR scene showing the same area. Here the motorway is heading in across-track. The flight direction is from bottom to the top and the scene is observed from the left side. On the upper part a fraction of the A96 can be seen. As the road is now heading in across-track moving vehicles are displaced from the road. The part of the azimuth line marked in the red area was taken from every of the differently processed images and the resulting FM-azimuth slice can be seen in Fig. 9. The red circles mark the two detected peaks.

Figure 5. SAR image with coloured rectangles, each marking an azimuth line used for building a FM-azimuth slice

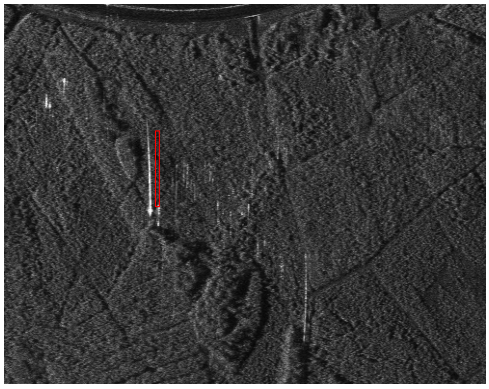

Figure 8. SAR image with red rectangle around the azimuth line used for building a FM-azimuth slice

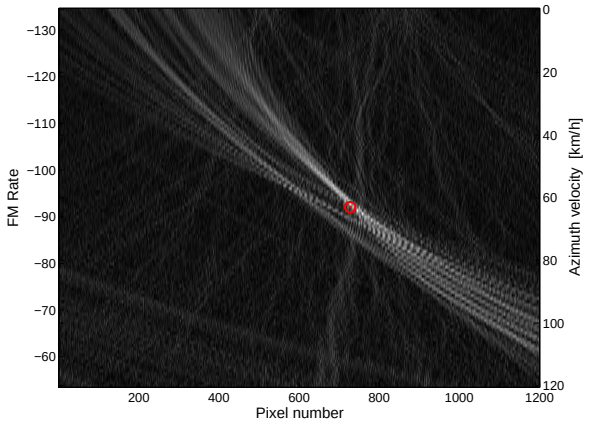

Figure 6. FM-azimuth sharpness function. Red circle marks the detected peak

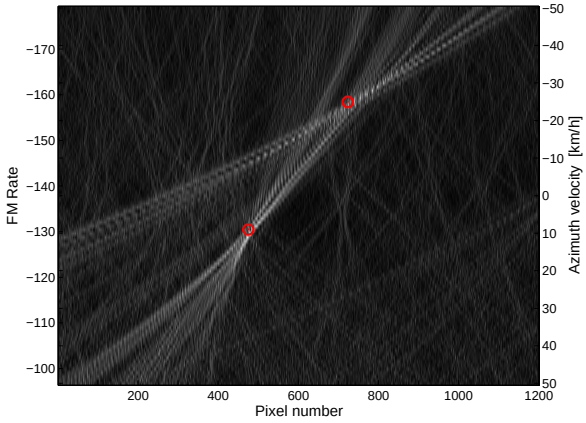

Figure 9. FM-azimuth sharpness function. Red circles mark the detected peaks

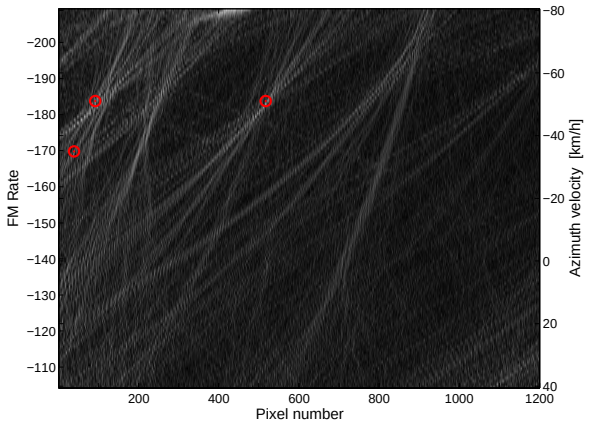

Figure 7. FM-azimuth sharpness function. Red circles mark the detected peaks

Due to the crosstalk of along-track motion and across-track acceleration the derivation of the along-track velocity directly from the FM-azimuth slices is not possible. The bias introduced by across-track acceleration can be examined by using the quadratic part of Equ. (5):

$$\frac{1}{2R_0}(\hat{v}_{x_0} - v_{sat})^2 = \frac{1}{2R_0}\left[(v_{x_0} - v_{sat})^2 + v_{y_0}^2\left(1 - \frac{y_0^2}{R_0^2}\right) + y_0 a_{y_0}\right] \tag{14}$$

Solving for $\hat{v}_{x_0}$ leads to:

$$\hat{v}_{x_0} = v_{sat} - \sqrt{(v_{x_0} - v_{sat})^2 + v_{y_0}^2\left(1 - \frac{y_0^2}{R_0^2}\right) + y_0 a_{y_0}} \tag{15}$$

It would be necessary to separate the across-track acceleration from the along-track motion to be able to estimate the velocity in azimuth. Theoretically it is possible to solve for across-track acceleration under certain assumptions in the cubic coefficient of the range history (Sharma *et al.*, 2006). However, along-track acceleration is dominant in the third-order coefficient.

Hence, the separation of both effects needs the adaption of external information. If a vehicle is detected redundant by different detectors, it may be possible to separate this effects by comparing the across-track velocity derived by using interferometric methods with the velocity estimated by the FM rate detector. Therefor a priori knowledge of the street direction out of the GIS data can be used. If successfully, the separation would provide beside the estimated velocity a sign for the acceleration, i.e. an additional parameter for traffic monitoring.

5. CONCLUSIONS AND FUTURE WORK

In this paper an approach was proposed to detect moving vehicles by exploiting the blurring effect due to along-track motion. The analysis with real data showed the capability of this technique.

In future improvements a combination with interferometric methods is aimed. False detections could be eliminated by considering redundant results of the different detection methods. Also the velocity estimation in along-track might be solvable by combining results of different detector schemes and integrating a priori information about the road network.

ACKNOWLEDGEMENTS

The authors would like to thank the DLR and the team of the TerraSAR-X traffic monitoring project for providing the E-SAR data to work with.

REFERENCES

Bamler, R. and Schättler, B., 1993. *SAR geocoding*, Chapter 3, pp. 53–102. Karlsruhe: Wichmann.

Ender, J., 1999. Space-time processing for multichannel synthetic aperture radar. *Electronics & Communication Engineering Journal* 11(1), 29–38.

Gierull, C., 2002. Moving Target Detection with Along-Track SAR Interferometry. Technical Report DRDC-OTTAWA-TR-2002-084, Defence Research & Development Canada.

Gierull, C. and Sikaneta, I., 2004. Ground Moving Target Parameter Estimation for Two-Channel SAR. In *EuSAR 2004 5th European Conference on Synthetic Aperture Radar*, Ulm, Germany. VDE.

Hinz, S., 2005. Fast and Subpixel Precise Blob Detection and Attribution. In *Proceedings of ICIP 05*.

Hinz, S., Meyer, F., Laika, A., and Bamler, R., 2005. Spaceborne traffic monitoring with dual channel synthetic aperture radar - theory and experiments. In *Proceedings of CVPR'05 Conference, San Diego*.

Meyer, F., Hinz, S., Laika, A., and Bamler, R., 2005. A-priori Information Driven Detection of Moving Objects for Traffic Monitoring by Spaceborne SAR. In *ISPRS-Workshop CMRT 05 "City Models, Road Databases, and Traffic Monitoring - Concepts, Algorithms, and Evaluations", Vienna*.

Sharma, J., Gierull, C., and Collins, M., 2006. The influence of target acceleration on velocity estimation in dual-channel SAR-GMTI. *IEEE Transactions on Geoscience and Remote Sensing* 44(1), 134–147.

Sikaneta, I. and Gierull, C., 2005. Two-Channel SAR Ground Moving Target Indication for Traffic Monitoring in Urban Terrain. In *Proc. of CMRT05, International Archives of Photogrammetry, Remote Sensing and Spatial Information Sciences*, Volume XXXVI, pp. 95–101.